Original Research *Feature article*

Silencing PSME3 induces colorectal cancer radiosensitivity by downregulating the expression of cyclin B1 and CKD1

Wen Song[1,2,3], Cuiping Guo[4], Jianxiong Chen[1,2], Shiyu Duan[1,2], Yukun Hu[1,2], Ying Zou[5], Honggang Chi[5], Jian Geng[1,2] and Jun Zhou[1,2]

[1]Department of Pathology, Nanfang Hospital, Southern Medical University, Guangzhou 510515, China; [2]Department of Pathology, School of Basic Medical Sciences, Southern Medical University, Guangzhou 510515, China; [3]Department of Radiotherapy, Nanfang Hospital, Southern Medical University, Guangzhou 510515, China; [4]Department of Emergency, Zhumadian Second Hospital of Traditional Chinese Medicine, Zhumadian 463000, China; [5]Department of Traditional Chinese Medicine, Scientific Research Platform, The Second School of Clinical Medicine, Guangdong Medical University, Dongguan 523808, China
Co-corresponding authors: Jian Geng and Jun Zhou. Email: geng@fimmu.com and chuhang127@163.com

Impact statement

It is reported that colorectal cancer (CRC) is the third most common cancer worldwide and the fourth leading cause of cancer-related death. At present, the main treatment method of colorectal cancer is surgery, supplemented by radiotherapy and chemotherapy. Among them, radiotherapy plays an important role in the treatment of locally advanced colorectal cancer, surgery, and chemotherapy. Our study found that down-regulation of PSME3 may enhance the radiosensitivity of CRC cells by triggering cell cycle arrest, which suggests that silence PSME3 may provide a new method for improving the radiosensitivity of CRC. What'more, our research also demonstrated that PSME3 may promote proliferation, invasive and migratory potential of CRC cells, which implies that PSME3 might be a biomarker of CRC for early diagnosis and treatment.

Abstract

Resistance to radiotherapy remains a severe obstacle in the treatment of high-risk colorectal cancer patients. Recent studies have indicated that proteasome activator complex subunit 3 (PSME3) participates in the development and progression of various human malignancies and is proposed to play a role in tumor radioresistance. However, the impact of PSME3 on radioresistance of colorectal cancer has been largely unknown. In the present study, the enhanced expression of PSME3 was observed in colorectal cancer cells and tissue. Upregulation of PSME3 was significantly implicated in lymph node state, lymphovascular invasion, and Dukes' stage. Furthermore, high PSME3 expression was closely linked to poorer overall and progression-free survival in patients with colorectal cancer. The study further demonstrated that the proliferative, invasive and migratory potential of colorectal cancer cells was effectively inhibited *in vitro* after silencing PSME3. Our results verified that knockdown of PSME3 probably triggered cell cycle arrest at the G2/M phase by downregulation of cyclinB1 and CDK1, thereby enhancing the radiosensitivity of colorectal cancer cells. These data illustrated that PSME3 is a promising biomarker predictive of colorectal cancer prognosis and silencing of PSME3 may provide with a new approach for sensitizing the radiotherapy in colorectal cancer.

Keywords: PSME3, colorectal cancer, cell cycle, radioresistance, proliferation, migration

Experimental Biology and Medicine **2019; 244: 1409–1418. DOI: 10.1177/1535370219883408**

Introduction

Colorectal cancer (CRC) remains one of the most pervasive malignancies worldwide, with its incidence and mortality rates progressively increasing.[1] Currently, radiotherapy plays a vital role in the treatment of locally advanced CRC, as well as surgery and chemotherapy. However, the existing combination therapy could hardly improve the high-risk CRC patients' overall survival partly due to chemoradiotherapy resistance. Therefore, it is desperately needed to explore new molecular biomarkers which can predict prognosis and therapy response for CRC patients.

PSME3 (proteasome activator complex subunit 3, namely REGγ or PA28γ), an important activator of the 20S proteasome, has been implicated in the regulation of the degradation of various key proteins, such as cell cycle inhibitors (p16, p19, p21, and p53) oncogenic steroid receptor coactivator-3 and ERα.[2–7] Amounting evidence has shown that overexpression of PSME3 frequently occurs in multiple kinds of human malignancies, including

pancreatic, oral, prostate, liver, breast, thyroid, endometrial cancer, and melanoma.[8–15] Roessler *et al.*[16] first indicated PSME3 as a novel serum biomarker for CRC. What's more, PSME3 has been involved in cell proliferation, apoptosis, and carcinogenesis.[17–19] PSME3-deficient mice displayed slow cell proliferation rate and small body size.[20] Blockade of PSME3 could inhibit cell proliferation and facilitate cell apoptosis.[21,22] These findings indicated a potential oncogenic role in tumorigenesis and cancer development. More importantly, depletion of PSME3 contributes to cellular radiomimetic sensitivity and a significant delay in DNA double-strand break (DSB) repair.[23] To date, nevertheless, the role of PSME3 in CRC radioresistance is not well elucidated.

In this study, PSME3 expression was higher in CRC cell lines and tissue relative to normal cells and tissue and significantly correlated with several aggressive clinicopathological parameters and unfavorable prognosis in CRC patients. Silencing of PSME3 significantly suppressed proliferation, invasion, and migration of CRC cells *in vitro*. We further demonstrated that PSME3 knockdown could induce G2/M phase cell cycle arrest by decreasing expression of cyclinB1 and CKD1 proteins, thereby enhancing the radiosensitivity of CRC cells.

Methods and materials

Cell culture

CRC cell lines Ls 174-T, Caco-2, HCT116, HT29, SW620, SW480, and LoVo were purchased from the American Type Culture Collection (ATCC). These cell lines were grown in RPMI 1640 medium (Gibco, Gaithersburg, MD, USA) with 10% fetal bovine serum (Gibco). They were cultured in a humidified 5% CO_2 atmosphere at 37°C.

Patients and tissue specimens

Paired 163 paraffin-embedded CRC and adjacent non-malignant colorectal tissue samples, as well as 6 pairs of fresh CRC and corresponding adjacent non-tumorous colorectal tissue, were collected from Nanfang Hospital, Southern Medical University (Guangzhou, China) between January 2004 and December 2008. These patients had not received any preoperative chemotherapy or radiotherapy. Their clinical data including gender, age, tumor site, tumor size, tumor differentiation, lymph node state, distant metastasis, lymphovascular invasion and Dukes' stage are shown in Table 1. Clinical staging of this disease was performed based on Dukes' classification. Detailed follow-up data were obtained from the outpatient records or by telephone. This study was approved by the Ethics Committee of Nanfang Hospital, Southern Medical University, and written informed consent was provided by all patients.

Western blotting

Total proteins were collected from tissue and cell lysates and then separated by SDS-polyacrylamide gel electrophoresis (PAGE) and electrotransferred onto a polyvinylidene difluoride (PVDF) membrane (Millipore Corp, Billerica, MA, USA). The membranes were blocked with 5% skimmed milk, followed by treatment with primary antibodies against PSME3, β-Tubulin, β-actin, Cyclin B1, and CDK1 (Cell signaling Technology, Beverly, MA). Then the membranes were incubated with secondary antibodies (anti-rabbit IgG, 1:5000 dilution, #7074, Cell Signaling). The signals were detected by enhanced chemiluminescence (Pierce, Rockford, IL, USA).

Quantitative real-time polymerase chain reaction

We utilized Trizol reagent (Invitrogen, Calsbad, CA) to extract total RNA from cultured cells and fresh tissue. cDNA synthesis was done by using the PrimeScript RT reagent Kit (Promega, Madison, WI, USA) according to the manufacturer's protocols. qPCR was carried out using the SYBR Premix EX Taq^{TM} (Takara, Dalian, China) and ABI 7500 Real-Time PCR system (Applied Biosystems, Foster City, USA). The primer sequences used to amplify PSME3 were as follows: 5′-AGAAGCGAAGGTTGGATGAGT-3′ (sense) and 5′-AGCCGGATCTCAGGTTTCACT-3′ (antisense). β-Tubulin was used as an endogenous control. Fold change was calculated by using the $2^{-\Delta\Delta CT}$ method.

Immunohistochemistry

One hundred and sixty-three paraffin-embedded CRC tissue and corresponding non-cancerous tissue were applied to perform immunohistochemistry (IHC). Briefly, tissue sections were rehydrated through graded alcohol. For antigen retrieval, the slides were immersed in sodium citrate buffer, followed by blocking the endogenous peroxidase activity with 3% hydrogen peroxide. Subsequently, the sections were incubated overnight at 4°C with the primary antibody against PSME3(1:500 dilution, Abcam, Cambridge, UK). After washing, the slides were treated with a secondary antibody (Cell Signaling, Danvers, MA, USA) at room temperature. After rinsing, they were stained with 3,3-diaminobenzidine (DAB), counterstained with Mayer's hematoxylin, dehydrated and mounted.

IHC evaluation

The immunostaining for PSME3 protein was scored by two independent pathologists based on the staining intensity and the proportion of PSME3-positive tumor cells. Briefly, the intensity was graded as 0 (negative), 1 (weak), 2 (medium), 3 (strong). The percent of positive cells was scored as "0" (0%), "1" (1–25%), "2" (26–50%), "3" (51–75%) and "4" (76–100%). A combined score was obtained by multiplying the intensity and proportion scores. Then the IHC score was classified as follow: "−" (score 0–2), "+" (score 3), "++" (score 4), and "+++" (score > 4). Finally, we divided 163 cases with CRC into low PSME3 expression group ("−", "+") and high PSME3 expression group ("++", "+++").

Lentiviral transfection

Short hairpin RNA (shRNA)-PSME3 was achieved by using the GV248 lentiviral vector (Genechem, Shanghai, China) according to the manufacturer's instructions.

Table 1. Relationship between PSME3 expression level and clinicalpathological parameters of CRC.

PSME3 expression					
Characteristics	***n*=163**	**Low (%)**	**High (%)**	***P* value**	χ^2
Gender				**0.355**	**0.855**
Male	102	46 (45.1)	56 (54.9)		
Female	61	23 (37.7)	38 (62.3)		
Age (years)				0.683	0.167
<54	81	33 (40.7)	48 (59.3)		
≥54	82	36 (43.9)	46 (56.1)		
Tumor site				0.971	0.060
Proximal colon	34	15 (44.1)	19 (55.9)		
	29	12 (41.4)	17 (58.6)		
Rectum	100	42 (42.0)	58 (58.0)		
Tumor size (cm)				0.207	1.591
<5	92	35 (38.0)	57 (62.0)		
≥5	71	34 (47.9)	37 (52.1)		
Tumor differentiation				0.394	1.863
Well	62	30 (48.4)	32 (51.6)		
Moderate	77	31 (40.3)	46 (59.7)		
Poor	24	8 (33.3)	16 (66.7)		
Lymph node state				0.005	7.964
Positive	63	18 (28.6)	45 (71.4)		
Negative	100	51 (51.0)	49 (49.0)		
Distant metastasis				0.083	3.008
Positive	26	7 (26.9)	19 (73.1)		
Negative	137	62 (45.3)	75 (54.7)		
Lymphovascular invasion				0.021	5.337
Positive	54	16 (29.6)	38 (70.4)		
Negative	109	53 (48.6)	56 (51.4)		
Dukes' stage				0.007	7.259
A+B	96	49 (51.0)	47 (49.0)		
C+D	67	20 (29.9)	47 (70.1)		

CRC: colorectal cancer.

The sequences of shRNA-PSME3 were: 5′- GGAGCUAGA CACAAUGAAATT -3′. Cells were collected for further studies after transfection.

CCK-8 proliferation assay

Cells were plated into 96-well plates at a density of 2×10^3 per well; 2–(2-Methoxy-4-nitrophenyl)-3–(4-nitrophenyl)-5–(2,4-disulfothenyl)-2H-tetrazolium salt (CCK-8, Dojindo, Rockville, USA) solution was added to per well. After 2 h, the absorbance of each well was recorded at 450 nm using a MicroplateAutoreader(Bio-Rad, Hercules, CA, USA).

Colony formation assay

Harvested cells were seeded in 6-well plates. After two weeks, the cells were washed twice with PBS before being fixed with methanol and stained with 1% crystal violet. The number of colonies containing ≥50 cells was counted under a microscope. The experiment was performed with three replicates.

Transwell invasion assay

Cells (2×10^5) suspended in serum-free medium were placed in the top chamber (Corning BioCoatMatrigel Invasion Chamber) with 8.0 μm PET Membrane. Culture medium containing 300 μL of 10% FBS was added to the lower chamber of the transwell. After 24 h of incubation, the cells were allowed to invade through the membrane to the lower surface. Finally, the cells were counted under a microscope in five randomly chosen fields (×200). The experiment was performed with three replicates.

Cell wound healing assay

For the wound healing assay, transfected SW480 or SW620 cells were seeded in 6-well tissue culture plates and incubated for 24 h. After three washes with cold PBS, scratch wounds were created by a 10 μL pipette tube. Cell migration was monitored for 48 h and photographs of wounds margins were taken under a microscope. Then the width of the scratch gap was measured.

Gene set enrichment analysis

To elucidate the potential mechanisms underlying PSME3-mediated CRC radioresistance, we performed GSEA by the Broad Institute GSEA version 4.0 software. The dataset GSE8671 containing 64 CRC tissue and matched normal colorectal tissue samples was downloaded from the NCBI's Gene Expression Omnibus (GEO, http://www.ncbi.nlm.nih.gov/geo/). The gene sets used for GSEA were obtained from the Molecular Signatures Database (MsigDB, http://software.broadinstitute.org/gsea/index.jsp).

The gene sets with a false discovery rate (FDR) less than 0.05 were considered as significantly enriched.

Cell cycle assay

After 24 h of irradiation, cells were harvested, washed with cold PBS, and fixed overnight at 4°C in 70% ethanol. After washing twice, these cells were stained with the Cell Cycle Detection Kit (KeyGen, Nanjing, China). Finally, the samples were collected and incubated with a buffer containing 50 μM propidium iodides (PI) in 37°C for 0.5 h and analyzed by flow cytometry (Becton–Dickinson, NJ, USA). The experiment was performed with three replicates.

Radiation sensitivity assays

Cells were seeded in 6-well plates at 2000 cells per well and incubated at 37°C with 5% CO_2 for clonogenic assay. To measure CRC radiosensitivity, the PSME3-negative cells (SW480/shPSME3 and SW620/shPSME3 cells) and the PSME3-positive cells (SW480 and SW620 cells) were treated with X-rays at different doses (2 Gy, 4 Gy, 6 Gy, 8 Gy), generated by a linear accelerator (Varian Clinac 23EX with 6 MeV photon irradiation at a dose rate of 5 Gy/min). At 10–14 days after irradiation, clones visible to the naked eye were washed, fixed, stained, and then calculated. Additionally, cell cycle distribution and cell cycle-related proteins (Cyclin B1 and CKD1) of CRC cells by treatment with 6 Gy of irradiation were estimated by cell cycle assay and Western blotting, respectively.

Statistical analysis

Data were analyzed by the SPSS 19.0 statistical software. Intergroup differences were analyzed using the Student's *t*-test. Significance of correlation between PSME3 expression and clinicopathological features was evaluated using Pearson's Chi-squared (χ^2) test. For survival analysis, the survival curves were plotted using the Kaplan–Meier method. The log-rank test was utilized to compare different survival curves. A P value less than 0.05 was considered statistically significant.

Results

PSME3 was upregulated in CRC cell lines and tissue

In order to determine the expression level of PSME3 in CRC cells, Western blotting and qPCR were employed to measure the expression of PSME3 in seven CRC cell lines including Ls 174-T, Caco-2, HCT116, HT29, SW620, SW480, and LoVo. Interestingly, PSME3 protein and mRNA were increased in Ls 174-T, SW620, and SW480, whereas decreased in HCT116, HT29 and LoVo (Figure 1 (a) and (c)). As described in Figure 1(b) and (d), fresh CRC tissue exhibited upregulated PSME3 protein and mRNA expression compared with corresponding normal tissue ($P < 0.05$). Furthermore, the results of IHC showed that positive staining for PSME3 was mainly located in the nucleus of CRC cells (Figure 2(a)), and enhanced PSME3 expression was witnessed in 94/163 (57.67%) of CRC tissue compared with corresponding adjacent non-cancerous tissue (Table 1).

Relationship between PSME3 expression and CRC patients' aggressive clinicopathological characters and prognosis

Clinical data from these 163 CRC patients were analyzed to evaluate the association between PSME3 expression and aggressive clinicopathological variables of CRC patients. High PSME3 expression was observed to be positively associated with lymph node state ($P = 0.005$),

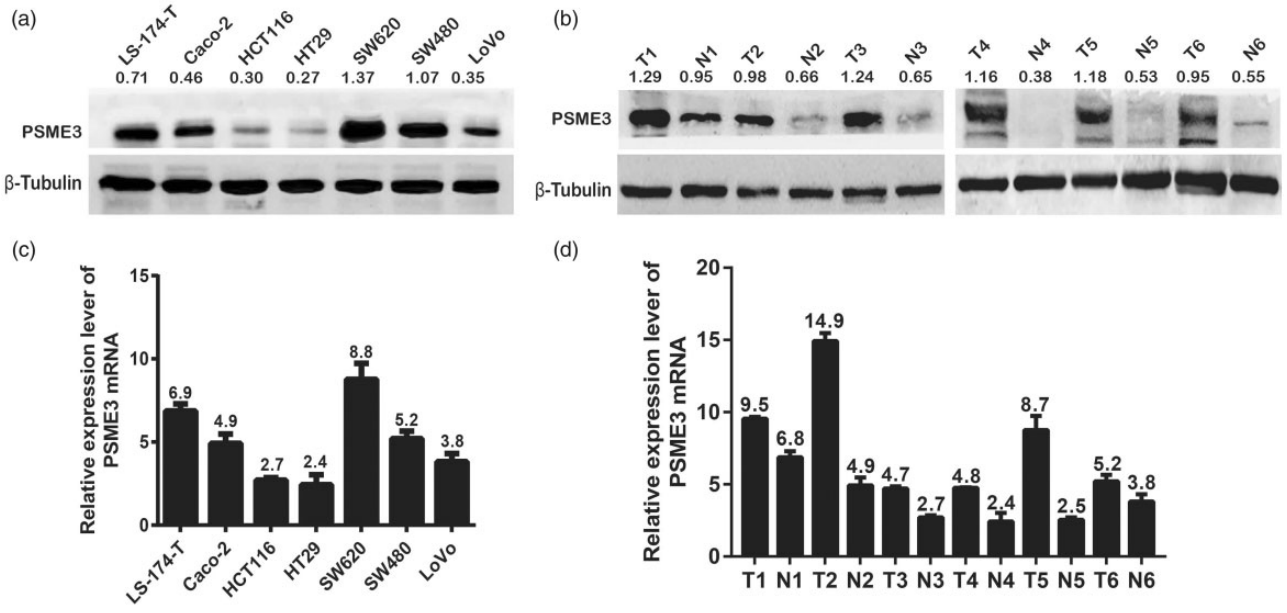

Figure 1. Expression of PSME3 in CRC cells and tissue. (a and c) The expression of PSME3 protein and mRNA in 7 CRC cell lines (Ls 174-T, Caco-2, HCT116, HT29, SW620, SW48, and LoVo) detected by Western blotting and qPCR. (b and d) The expression of PSME3 protein and mRNA in 6 pairs of fresh CRC and adjacent non-malignant tissue detected by Western blotting and qPCR.

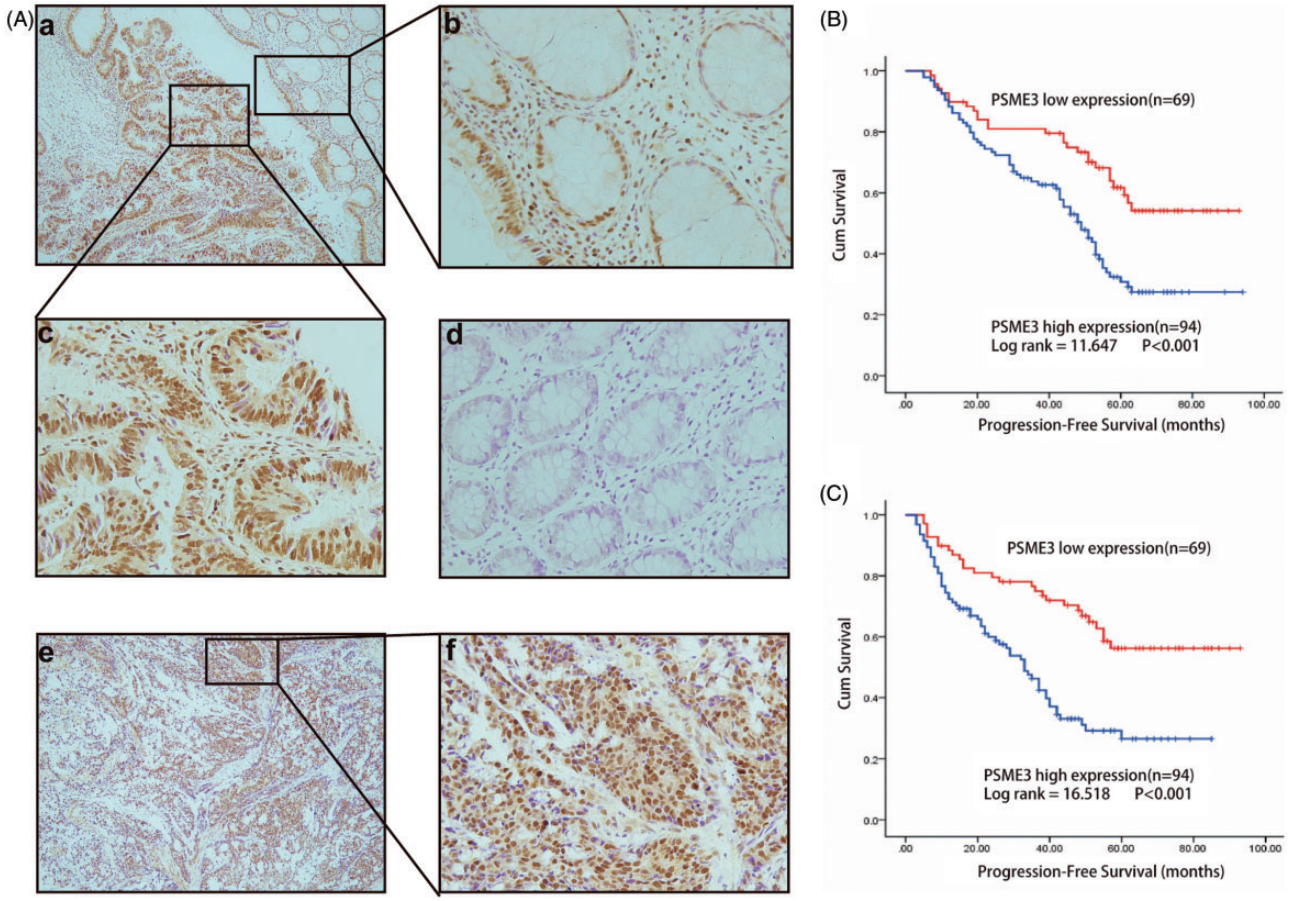

Figure 2. Upregulation of PSME3 predicted poor prognosis of CRC. (A) The expression of PSME3 protein by IHC: (a) Representative images of PSME3 expression in CRC and adjacent non-cancerous tissue (scale bar, 100 μm), (b) weak staining for PSME3 in paired adjacent normal tissue (scale bar, 20 μm), (c) strong staining for PSME3 in CRC tissue (scale bar, 20 μm), (d) negative staining for PSME3 in normal colorectal tissue, (e and f) strong staining for PSME3 in CRC tissue (scale bar, 100 μm and 20 μm). (B and C) The relationship between PSME3 expression in 163 CRC patients and overall survival or progression-free survival evaluated by Kaplan–Meier survival analysis.

lymphovascular invasion ($P = 0.021$), and Dukes' stage ($P = 0.007$) in CRC patients. However, no significant relationship was found between PSME3 expression and other clinicopathological parameters ($P > 0.05$; Table 1). More importantly, Kaplan–Meier survival analysis was performed to explore the correlation between PSME3 expression and the survival of CRC patients. The results indicated that overall survival ($P = 0.001$, Figure 2(b)) and progression-free survival ($P < 0.001$, Figure 2(c)) of high PSME3 expression group was shorter than that of low PSME3 expression group.

Silencing PSME3 inhibited proliferation, invasion, and migration of CRC cells

We next attempted to investigate whether knockdown of PSME3 could affect the proliferative, invasive, and migratory potential of CRC cells. Endogenous expression of PSME3 was silenced in SW480 and SW620 cells by using a lentiviral vector carrying a specific shRNA (Figure 3(a) and (b)). As shown in Figure 3(c) to (e), SW480/shPSME3 and SW620/shPSME3 cells displayed a weakened proliferation ability compared with the control group ($P < 0.05$). Moreover, downregulation of PSME3 could induce a dramatic decrease in the invasive and migratory capacity of PSME3-silenced cells ($P < 0.05$; Figure 3(f) to (h)). Collectively, these findings provide evidence that PSME3 promote the proliferation, invasion, and migration of CRC cells.

Effects of stable silencing PSME3 on the radioresistance of CRC cell lines

Colony formation assay was performed to analyze the effect of PSME3 on the radiosensitivity of CRC cells. As shown in Figure 4, the clonogenic capacity of the PSME3-negative (SW480/shPSME3 and SW620/shPSME3) cells was significantly reduced compared to that of the PSME3-positive (SW480/control and SW620/control) cells with different doses of irradiation, indicating an increased radiosensitivity after knockdown of PSME3 gene expression.

In order to investigate the molecular mechanisms by which PSME3 regulated CRC radioresistance, we performed gene set enrichment analysis (GSEA) to make comparisons of the gene expression profiles between PSME3low and PSME3high CRC specimens. Sixty-four CRC tissue samples derived from the TCGA database were divided into PSME3low ($n = 32$) and PSME3high ($n = 32$) groups based on the median PSME3 expression. The results of GSEA demonstrated that the gene set of

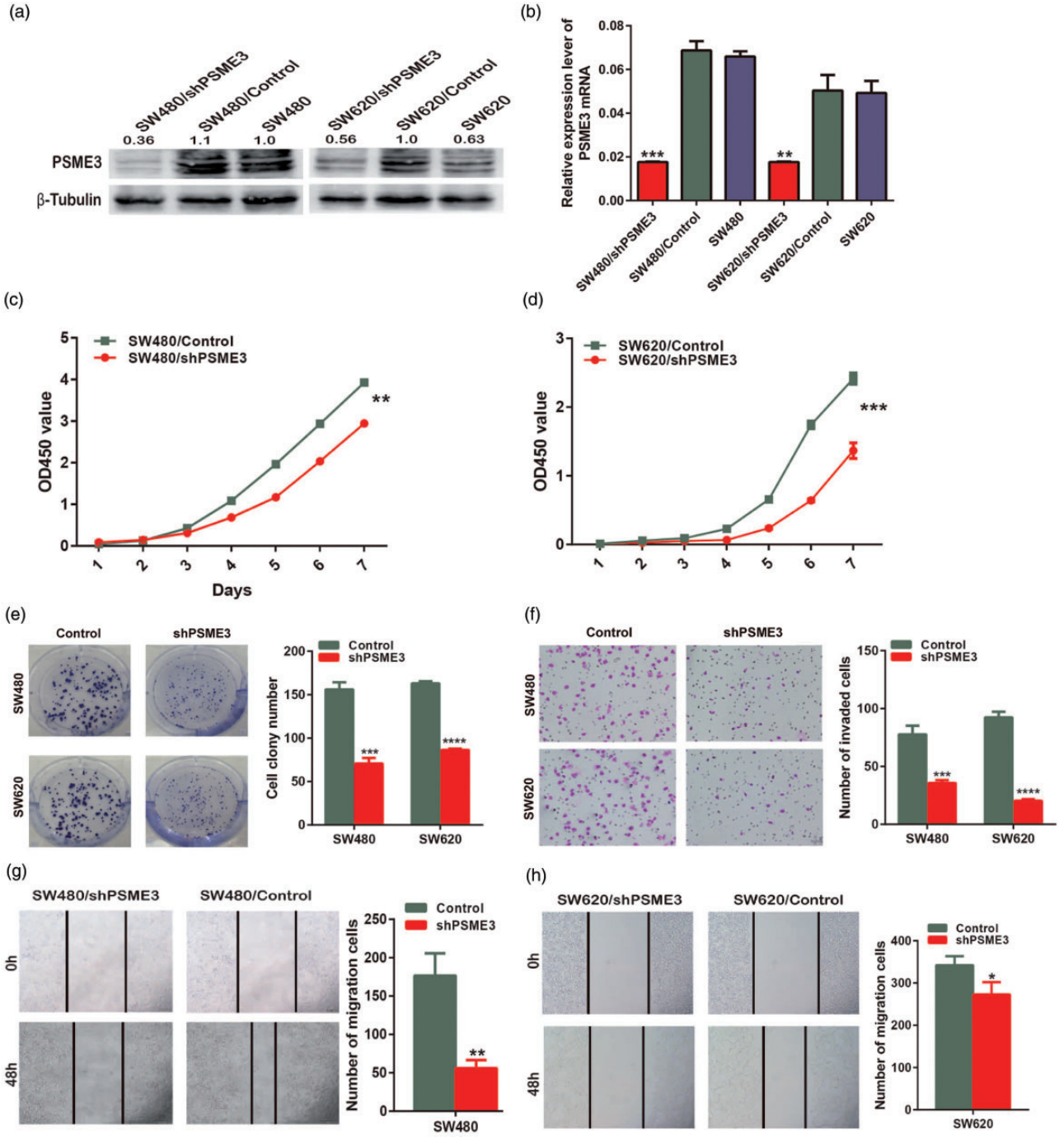

Figure 3. Effects of PSME3 inhibition on proliferation, migration, and invasion of CRC cells. (a and b) A significant reduction of PSME3 was achieved in SW480 and SW620 cells by Western blotting and qPCR. Mean ± SD ($n = 3$). (c, d, and e) Knockdown of PSME3 inhibited cell growth and proliferation as determined by CCK-8 proliferation and colony formation assays. Mean ± SD ($n = 3$). (f) PSME3 knockdown significantly suppressed the invasion ability was significantly lower in the PSME3-silenced cells than that in the control cells. Representative photographs (left) and quantification (right) are shown. The number of cells that invaded through the extracellular matrix after 24 h was counted in five randomly selected microscopic fields. Mean ± SD ($n = 3$). Scale bars, 100 μm. (g and h) The migration ability of the PSME3-silenced cells was significantly reduced compared with the control cells. Images were taken at 0 h, 24 h, and 48 h. A number of migrated cells was calculated (right). Mean ± SD ($n = 3$). Scale bars, 200 μm. *$P < 0.05$; **$P < 0.01$. (A color version of this figure is available in the online journal.)

KEGG_CELL_CYCLE (cell cycle)(Figure 5(a)) was highly enriched in PSME3high CRC specimens, which indicated that PSME3 might be involved in the regulation of cell cycle progression of CRC.

To validate this finding, cell cycle assay and Western blotting were further performed to respectively detect cell cycle distribution and cell cycle-related proteins' (Cyclin B1 and CKD1) expression of CRC cells after radiotherapy. We found that the PSME3-negative group contained a significantly higher percentage of cells at the G2/M phase of the cell cycle than the PSME3-positive group after irradiation by cell cycle assay (Figure 5(b)). More importantly, the results of Western blotting showed that the expression of cyclinB1 and CKD1 protein in the

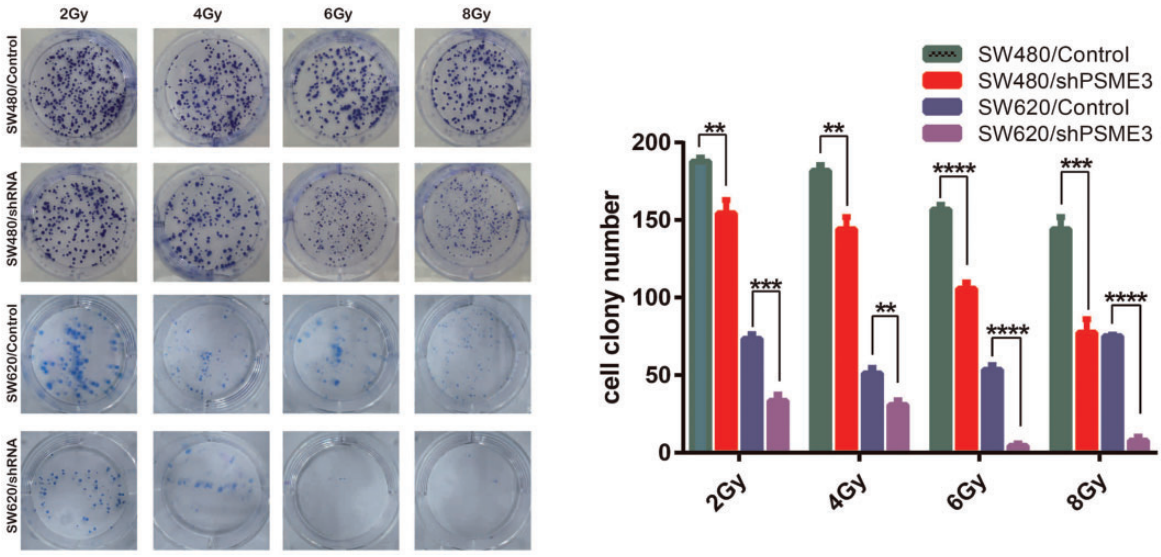

Figure 4. The impacts of silencing PSME3 on the radioresistance of CRC cells. The clonogenic capacity of the PSME3-negative (SW480/shPSME3 and SW620/shPSME3) cells was significantly reduced compared to that of the PSME3-positive (SW480/control and SW620/control) cells when respectively exposed to different doses of irradiation. $^{**}P < 0.01$; $^{***}P < 0.001$; $^{****}P < 0.0001$. (A color version of this figure is available in the online journal.)

PSME3-negative cells was significantly decreased compared with that in the PSME3-positive cells after radiotherapy (Figure 5(c)). These observations suggest that knockdown of PSME3 may induce the radiosensitivity of CRC cells by modulating the expression of cell cycle-related proteins Cyclin B1 and CKD1.

Discussion

Previous studies have demonstrated that upregulation of PSME3 is implicated in aggressive characteristics and unfavorable prognosis of various human cancers.[8,11] It is also reported that the expression of PSME3 in CRC tissue was significantly higher than that in normal tissue.[16] And our study that PSME3 was markedly elevated in CRC occurred with the previous work. Meanwhile, we also found that PSME3 closely linked to several aggressive clinicopathological variables of CRC patients, including lymph node state, lymphovascular invasion, and Dukes' stage. Importantly, those CRC patients with high expression of PSME3 had a poorer prognosis than those exhibiting low expression of PSME3, consistent with the previous observation.[21] Further studies demonstrated that depletion of PSME3 could inhibit the proliferation, invasion, and migration of CRC cells *in vitro*. These findings provide compelling evidence that overexpression of PSME3 closely correlates with CRC progression and poor prognosis, suggesting that it will be a promising prognostic marker and therapeutic target for CRC.

Radioresistance poses a major clinical challenge in the effective treatment of locally advanced CRC. Multiple lines of evidence supported the notion that the resistance to radiotherapy closely correlated with cell cycle arrest, cancer stem cells, tumor microenvironment change, and other factors.[24–28] Thus, exploring the potential mechanisms of CRC radioresistance and searching for effective therapeutic methods will help us improve the effect of radiotherapy. By colony-forming assay, we first found that the clonogenic capability of PSME3-negative cells was significantly inhibited compared with that of PSME3-positive cells when respectively exposed to different doses of irradiation, indicating that silencing of PSME3 could lead to the radiosensitivity of CRC cells.

Recently, cell cycle arrest has been of great interest to oncologists due to hindering tumor cells from radiation-induced damage. The radiobiological theory has elucidated that the radiosensitivity of cells differs at each phase of the cell cycle. Pauwels *et al.*[29] demonstrated that cells at the G2 and M phases of the cell cycle are more sensitive to ionizing radiation, whereas those at the S and G0 phases are less sensitive. Studies conducted by Deng YR *et al.*[30–32] validated that the G2/M phase cell cycle arrest induced the radioresistance of multiple malignant cells. Furthermore, cervical cancer radioresistance could be attenuated by inducing cell cycle arrest at the G2/M phase.[33] The results provide a rationale to support the speculation that radiosensitivity will be enhanced when cells arrest at the G2/M phase. Using bioinformatics analysis, the gene set related to the cell cycle was found to be positively associated with upregulated PSME3 expression. Several studies demonstrated that PSME3 has been implicated in the regulation of cell cycle progression.[4,34] These findings drove us to hypothesize that PSME3 might affect radiotherapy response by induction of cell cycle arrest. In the present study, we performed cell cycle assay to verify that the proportion of G2/M phase cells was increased in both the PSME3-negative and PSME3-positive cells after irradiation. Of note, the percentage of irradiated PSME3-negative cells at G2/M phase was apparently higher than that of irradiated PSME3-positive cells, validating the results as a proof that silencing PSME3 induces G2/M phase arrest of the cell cycle after irradiation. Taken together, the above

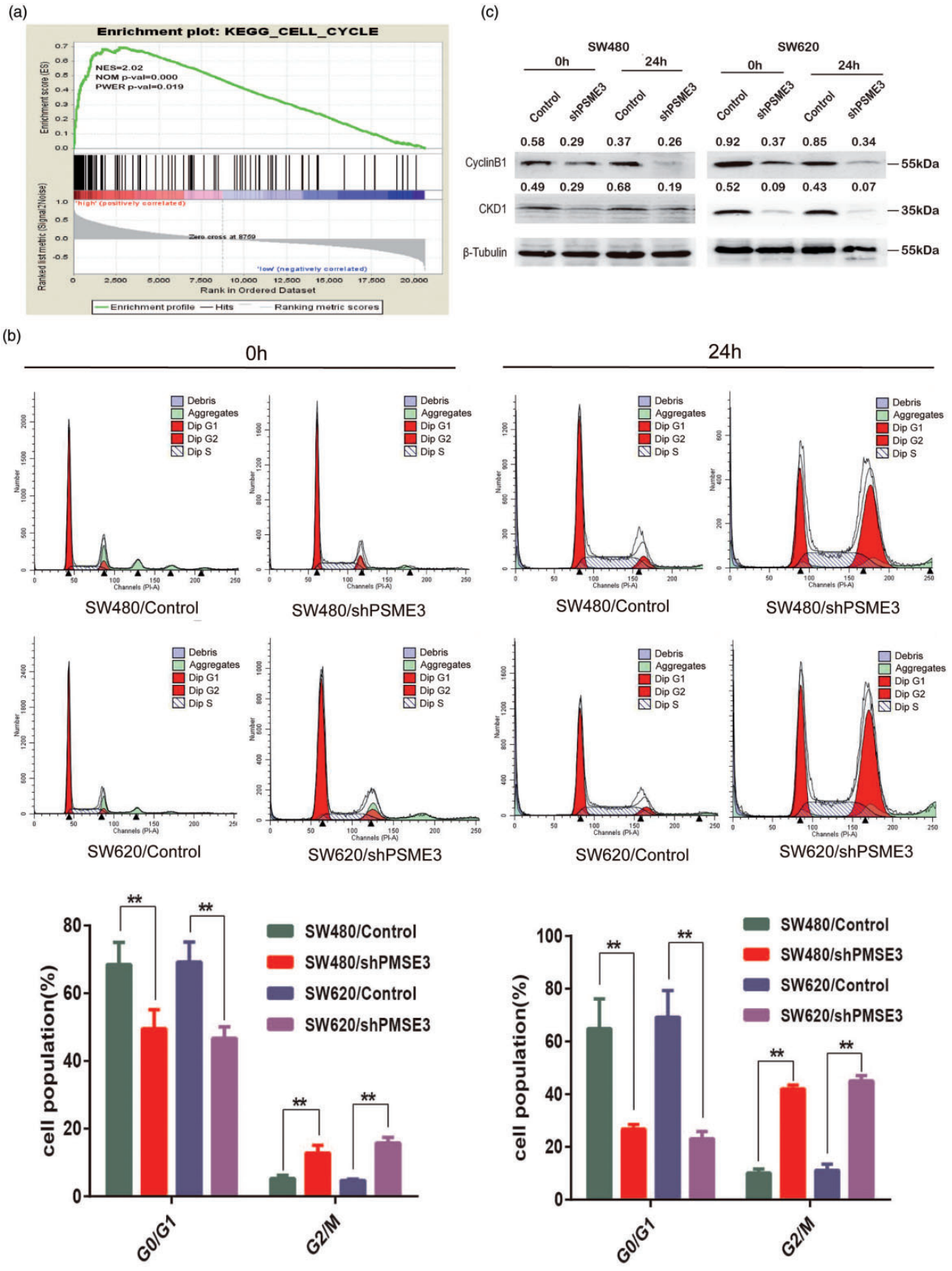

Figure 5. The impacts of silencing PSME3 on the cell-cycle progression and cell-cycle-related proteins of CRC cells. (a) Gene set of CELL_CYCLE is positively associated with high PSME3 expression in CRC by gene set enrichment analysis (GSEA). The value at the peak is the enrichment score for a gene set, whereas the lower part shows the value of the ranking metric as it moves down the list of the ranked genes. Y-axis: the value of the ranking metric; X-axis: the rank for all genes. NES: normalized enrichment score; FWER: family-wise error rate. (b) The PSME3-negative group displayed a significantly higher percentage of cells at the G2/M phase of the cell cycle than the PSME3-positive group after irradiation by cell cycle assay. $^{*}P < 0.05$; $^{**}P < 0.01$. (c) Expression of cyclin B1 and CDK1 proteins in the control group and PSME3-negative cells was determined by Western blotting. β-actin was used as a loading control. (A color version of this figure is available in the online journal.)

observations indicate that knockdown of PSME3 probably enhances the radiosensitivity by regulating cell cycle transition of CRC cells.

Accumulating data has shown that cell cycle progression is controlled by members of cyclin and cyclin-dependent kinases (CDKs).[35–37] Cyclin B1 was known as a member of the cyclin family and involved in the regulation of the G2/M phase transition.[38,39] A study by Hartwell *et al.*[40] demonstrated that upregulation of Cyclin B1 protein could promote G2/M phase transition, thereby resulting in uncontrolled cell proliferation and malignant transformation. Overexpression of transcriptional factor c-Myb might facilitate the expression of Cyclin B1, thereby promoting the G2/M phase transition.[41] Stable silencing of cyclin B1 in tumor cells induced the G2/M phase arrest.[42] Cyclin-dependent kinases (CDKs) are the catalytic subunits of a family of mammalian heterodimeric serine/threonine protein kinases.[43,44] During the G2/M phase of the cell cycle, cyclin-dependent protein kinase 1 (CDK1) triggers entry into mitosis when bound to cyclinB1.[45] Downregulation of cyclinB1/CDK1 resulted in G2/M cell cycle arrest in pancreatic cancer cells.[46] These findings demonstrated that cell cycle arrest will occur at G2/M phase when Cyclin B1 and CDK1 proteins are down-regulated.

To further investigate the possible mechanism by which PSME3 mediated G2/M phase cell cycle arrest in CRC radioresistance, we measured the expression level of Cyclin B1 and CDK1 proteins. In this study, we found that expression of CyclinB1 and CDK1 in the irradiated PSME3-negative cells was significantly lower than in the irradiated PSME3-positive cells, which would contribute to a more significant reduction in the formation of cyclin B1-CDK1 complexes, accompanied by a more significant increase in the number of G2/M phase cells. These results demonstrate that knockdown of PSME3 induces the G2/M phase cell cycle arrest probably by down-regulating CyclinB1 and CDK1, thereby enhancing radiosensitivity of CRC cells. However, further studies should be performed to fully explore the precise mechanisms of CRC radioresistance.

In conclusion, we have highlighted that PSME3 upregulation is observed in CRC and can predict poor prognosis of CRC patients. Our study further verified that knockdown of PSME3 can suppress the proliferative, invasive and migratory potential of CRC cells. Furthermore, knockdown of PSME3 is capable of inducing the G2/M phase cell arrest by downregulating the expression of cyclinB1 and CKD1, thereby enhancing the radiosensitivity of CRC cells. These present findings reveal that PSME3 will be a promising and valuable biomarker for predicting the radiosensitivity of CRC cells.

Authors' contributions: JZ and JG led study design and prepared the manuscript; W S carried out the experiments; CG performed statistical analysis; JC assisted in tissue sample collection; SD and YH performed data analysis and interpretation; YZ and HC provided data collection All authors read and approved the final manuscript.

DECLARATION OF CONFLICTING INTERESTS

The author(s) declared no potential conflicts of interest with respect to the research, authorship, and/or publication of this article.

FUNDING

This study was supported by the National Natural Science Foundation of China (grant no. 81272763 and 81672466), the Natural Science Foundation of Guangdong Province (grant no. 2014A030313286 and 2017A030313550) And "Group-type" Special Support Project for Education Talents in Universities (grant no. G619080438 and 4SG19044G).

ORCID iD

Jun Zhou https://orcid.org/0000-0002-1807-2606

REFERENCES

1. Torre LA, Bray F, Siegel RL, Ferlay J, Lortet-Tieulent J, Jemal A. Global cancer statistics, 2012. *CA Cancer J Clin* 2015;**65**:87–108
2. Chai F, Liang Y, Bi J, Chen L, Zhang F, Cui Y, Jiang J. REGgammaregulatesERalpha degradation via a ubiquitin-proteasome pathway in breast cancer. *Biochem Biophys Res Commun* 2015;**456**:534–40
3. Kobayashi T, Wang J, Al-Ahmadie H, Abate-Shen C. ARF regulates the stability of p16 protein via REGgamma-dependent proteasome degradation. *Mol Cancer Res* 2013;**11**:828–33
4. Ali A, Wang Z, Fu J, Ji L, Liu J, Li L, Wang H, Chen J, Caulin C, Myers JN, Zhang P, Xiao J, Zhang B, Li X. Differential regulation of the REGgamma-proteasome pathway by p53/TGF-beta signalling and mutant p53 in cancer cells. *Nat Commun* 2013;**4**:2667
5. Chen X, Barton LF, Chi Y, Clurman BE, Roberts JM. Ubiquitin-independent degradation of cell-cycle inhibitors by the REGgamma proteasome. *Mol Cell* 2007;**26**:843–52
6. Li X, Amazit L, Long W, Lonard DM, Monaco JJ, O'Malley BW. Ubiquitin- and ATP-independent proteolytic turnover of p21 by the REGgamma-proteasome pathway. *Mol Cell* 2007;**26**:831–42
7. Li X, Lonard DM, Jung SY, Malovannaya A, Feng Q, Qin J, Tsai SY, Tsai MJ, O'Malley BW. The SRC-3/AIB1 coactivator is degraded in a ubiquitin- and ATP-independent manner by the REGgamma proteasome. *Cell* 2006;**124**:381–92
8. Guo J, Hao J, Jiang H, Jin J, Wu H, Jin Z, Li Z. Proteasome activator subunit 3 promotes pancreatic cancer growth via c-Myc-glycolysis signaling axis. *Cancer Lett* 2017;**386**:161–7
9. Chen S, Wang L, Xu C, Chen H, Peng B, Xu Y, Yao X, Li L, Zheng J. Knockdown of REGgamma inhibits proliferation by inducing apoptosis and cell cycle arrest in prostate cancer. *Am J Transl Res* 2017;**9**:3787–95
10. Chen H, Gao X, Sun Z, Wang Q, Zuo D, Pan L, Li K, Chen J, Chen G, Hu K, Li K, Shah AS, Huang T, Muhammad Zeeshan B, Tong L, Jiao C, Liu J, Chen T, Yao L, Dang Y, Liu T, Li L. REGgamma accelerates melanoma formation by regulating Wnt/beta-catenin signalling pathway. *Exp Dermatol* 2017;**26**:1118–24
11. Li J, Feng X, Sun C, Zeng X, Xie L, Xu H, Li T, Wang R, Xu X, Zhou X, Zhou M, Zhou Y, Dan H, Wang Z, Ji N, Deng P, Liao G, Geng N, Wang Y, Zhang D, Lin Y, Ye L, Liang X, Li L, Luo G, Jiang L, Wang Z, Chen Q. Associations between proteasomal activator PA28gamma and outcome of oral squamous cell carcinoma: evidence from cohort studies and functional analyses. *EBioMedicine* 2015;**2**:851–8
12. Wang H, Bao W, Jiang F, Che Q, Chen Z, Wang F, Tong H, Dai C, He X, Liao Y, Liu B, Sun J, Wan X. Mutant p53 (p53-R248Q) functions as an oncogene in promoting endometrial cancer by up-regulating REGgamma. *Cancer Lett* 2015;**360**:269–79
13. He J, Cui L, Zeng Y, Wang G, Zhou P, Yang Y, Ji L, Zhao Y, Chen J, Wang Z, Shi T, Zhang P, Chen R, Li X. REGγ is associated with multiple oncogenic pathways in human cancers. *BMC Cancer* 2012;**12**:75

14. Zhang M, Gan L, Ren GS. REGgamma is a strong candidate for the regulation of cell cycle, proliferation and the invasion by poorly differentiated thyroid carcinoma cells. *Braz J Med Biol Res* 2012;**45**:459–65
15. Wang X, Tu S, Tan J, Tian T, Ran L, Rodier JF, Ren G. REG gamma: a potential marker in breast cancer and effect on cell cycle and proliferation of breast cancer cell. *Med Oncol* 2011;**28**:31–41
16. Roessler M, Rollinger W, Mantovani-Endl L, Hagmann ML, Palme S, Berndt P, Engel AM, Pfeffer M, Karl J, Bodenmüller H, Rüschoff J, Henkel T, Rohr G, Rossol S, Rösch W, Langen H, Zolg W, Tacke M. Identification of PSME3 as a novel serum tumor marker for colorectal cancer by combining two-dimensional polyacrylamide gel electrophoresis with a strictly mass spectrometry-based approach for data analysis. *Mol Cell Proteomics* 2006;**5**:2092–101
17. Moncsek A, Gruner M, Meyer H, Lehmann A, Kloetzel PM, Stohwasser R. Evidence for anti-apoptotic roles of proteasome activator 28gamma via inhibiting caspase activity. *Apoptosis* 2015;**20**:1211–28
18. Tanaka K. The proteasome: overview of structure and functions. *Proc Jpn Acad Ser B* 2009;**85**:12–36
19. Mao I, Liu J, Li X, Luo H. REGgamma, a proteasome activator and beyond? *Cell Mol Life Sci* 2008;**65**:3971–80
20. Murata S, Kawahara H, Tohma S, Yamamoto K, Kasahara M, Nabeshima Y, Tanaka K, Chiba T. Growth retardation in mice lacking the proteasome activator PA28gamma. *J Biol Chem* 1999;**274**:38211–5
21. Chen S, Wang Q, Wang L, Chen H, Gao X, Gong D, Ma J, Kubra S, Yao X, Li X, Li L, Zhai W, Zheng J. REGγ deficiency suppresses tumor progression via stabilizing CK1ε in renal cell carcinoma. *Cell Death Dis* 2018;**9**:627
22. Barton LF, Runnels HA, Schell TD, Cho Y, Gibbons R, Tevethia SS, Deepe GJ, Monaco JJ. Immune defects in 28-kDa proteasome activator gamma-deficient mice. *J Immunol* 2004;**172**:3948–54
23. Levy-Barda A, Lerenthal Y, Davis AJ, Chung YM, Essers J, Shao Z, van Vliet N, Chen DJ, Hu MC, Kanaar R, Ziv Y, Shiloh Y. Involvement of the nuclear proteasome activator PA28gamma in the cellular response to DNA double-strand breaks. *Cell Cycle* 2011;**10**:4300–10
24. Campbell RM, Anderson BD, Brooks NA, Brooks HB, Chan EM, De Dios A, Gilmour R, Graff JR, Jambrina E, Mader M, McCann D, Na S, Parsons SH, Pratt SE, Shih C, Stancato LF, Starling JJ, Tate C, Velasco JA, Wang Y, Ye XS. Characterization of LY2228820 dimesylate, a potent and selective inhibitor of p38 MAPK with antitumor activity. *Mol Cancer Ther* 2014;**13**:364–74
25. Wang Y, Yin W, Zhu X. Blocked autophagy enhances radiosensitivity of nasopharyngeal carcinoma cell line CNE-2 in vitro. *Acta Otolaryngol* 2014;**134**:105–10
26. Li J, Yang CX, Mei ZJ, Chen J, Zhang SM, Sun SX, Zhou FX, Zhou YF, Xie CH. Involvement of cdc25c in cell cycle alteration of a radioresistant lung cancer cell line established with fractionated ionizing radiation. *Asian Pac J Cancer Prev* 2013;**14**:5725–30
27. Kuballa P, Nolte WM, Castoreno AB, Xavier RJ. Autophagy and the immune system. *Annu Rev Immunol* 2012;**30**:611–46
28. Al-Ejeh F, Smart CE, Morrison BJ, Chenevix-Trench G, Lopez JA, Lakhani SR, Brown MP, Khanna KK. Breast cancer stem cells: treatment resistance and therapeutic opportunities. *Carcinogenesis* 2011;**32**:650–8
29. Pauwels B, Wouters A, Peeters M, Vermorken JB, Lardon F. Role of cell cycle perturbations in the combination therapy of chemotherapeutic agents and radiation. *Future Oncol* 2010;**6**:1485–96
30. Deng YR, Chen XJ, Chen W, Wu LF, Jiang HP, Lin D, Wang LJ, Wang W, Guo SQ. Sp1 contributes to radioresistance of cervical cancer through targeting G2/M cell cycle checkpoint CDK1. *Cancer Manag Res* 2019;**11**:5835–5844
31. Ross Carruthers, Shafiq U. Ahmed, Karen Strathdee, Natividad Gomez-Roman, Evelyn Amoah-Buahin, Colin Watts, Anthony J. Chalmers. Abrogation of radioresistance in glioblastoma stem-like cells by inhibition of ATM kinase. *Mol Oncol* 2015;**9**;192–203
32. Gogineni VR, Nalla AK, Gupta R, Dinh DH, Klopfenstein JD, Rao JS. Chk2-mediated G2/M cell cycle arrest maintains radiation resistance in malignant meningioma cells. *Cancer Lett* 2011;**313**:64–75
33. Ju X, Liang S, Zhu J, Ke G, Wen H, X W. Extracellular matrix metalloproteinase inducer (CD147/BSG/EMMPRIN)-induced radioresistance in cervical cancer by regulating the percentage of the cells in the G2/m phase of the cell cycle and the repair of DNA double-strand breaks (DSBs). *Am J Transl Res* 2016;**8**:2498–511
34. Shi Y, Luo X, Li P, Tan J, Wang X, Xiang T, Ren G. miR-7-5p suppresses cell proliferation and induces apoptosis of breast cancer cells mainly by targeting REGγ. *Cancer Lett* 2015;**358**:27–36
35. Liu Y, Wang W, Fang B, Ma F, Zheng Q, Deng P, Zhao S, Chen M, Yang G, He G. Anti-tumor effect of germacrone on human hepatoma cell lines through inducing G2/M cell cycle arrest and promoting apoptosis. *Eur J Pharmacol* 2013;**698**:95–102
36. Huang WW, Ko SW, Tsai HY, Chung JG, Chiang JH, Chen KT, Chen YC, Chen HY, Chen YF, Yang JS. Cantharidin induces G2/M phase arrest and apoptosis in human colorectal cancer colo 205 cells through inhibition of CDK1 activity and caspase-dependent signaling pathways. *Int J Oncol* 2011;**38**:1067–73
37. Gavet O, Pines J. Progressive activation of CyclinB1-Cdk1 coordinates entry to mitosis. *Dev Cell* 2010;**18**:533–43
38. Badie C, Bourhis J, Sobczak-Thepot J, Haddada H, Chiron M, Janicot M, Janot F, Tursz T, Vassal G. p53-dependent G2 arrest associated with a decrease in cyclins A2 and B1 levels in a human carcinoma cell line. *Br J Cancer* 2000;**82**:642–50
39. Evans T, Rosenthal ET, Youngblom J, Distel D, Hunt T. Cyclin: a protein specified by maternal mRNA in sea urchin eggs that is destroyed at each cleavage division. *Cell* 1983;**33**:389–96
40. Hartwell LH, Kastan MB. Cell cycle control and cancer. *Science* 1994;**266**:1821–8
41. Nakata Y, Shetzline S, Sakashita C, Kalota A, Rallapalli R, Rudnick SI, Zhang Y, Emerson SG, Gewirtz AM. c-Myb contributes to G2/M cell cycle transition in human hematopoietic cells by direct regulation of cyclin B1 expression. *Mol Cell Biol* 2007;**27**:2048–58
42. Yuan J, Kramer A, Matthess Y, Yan R, Spankuch B, Gatje R, Knecht R, Kaufmann M, Strebhardt K. Stable gene silencing of cyclin B1 in tumor cells increases susceptibility to taxol and leads to growth arrest in vivo. *Oncogene* 2006;**25**:1753–62
43. Malumbres M, Barbacid M. Cell cycle kinases in cancer. *Curr Opin Genet Dev* 2007;**17**:60–5
44. Shapiro GI. Cyclin-dependent kinase pathways as targets for cancer treatment. *J Clin Oncol* 2006;**24**:1770–83
45. Astrinidis A, Senapedis W, Coleman TR, Henske EP. Cell cycle-regulated phosphorylation of hamartin, the product of the tuberous sclerosis complex 1 gene, by cyclin-dependent kinase 1/cyclin B. *J Biol Chem* 2003;**278**:51372–9
46. Feng W, Cai D, Zhang B, Lou G, Zou X. Combination of HDAC inhibitor TSA and silibinin induces cell cycle arrest and apoptosis by targeting surviving and cyclinB1/Cdk1 in pancreatic cancer cells. *Biomed Pharmacother* 2015;**74**:257–64

(Received August 15, 2019, Accepted September 26, 2019)